

29 **Synopsis:** Supercritical CO₂ with minimal co-solvents regenerates PFOA-laden GAC with > 99.9%
30 desorption efficiency.

31 **1 Introduction**

32 Granular activated carbon (GAC) is used to treat contaminated waters with per- and
33 polyfluoroalkyl substances (PFAS).¹ While widespread adoption of GAC offers a cost-effective
34 solution, it also creates a pressing need for managing the accumulation of spent GAC. Sorbent
35 regeneration unlocks the potential for sustainable, large-scale treatment of PFAS-contaminated
36 streams.² Thermal regeneration utilizes high temperatures, ~600-1000°C, to desorb PFAS and
37 other contaminants. The higher temperatures can also effectively destroy PFAS in situ; however,
38 the process is energy-demanding and can lead to GAC degradation and loss.³ Recent studies also
39 show that thermal degradation yields the formation of volatile organo-fluorine (VOF)
40 compounds that could re-enter the environment as gases or aerosols.⁴

41 Motivated by the development of various end-of-life PFAS destruction technologies^{5, 6}, the
42 effective PFAS transport from sorbents into concentrated liquid feedstock becomes highly
43 desirable. Approaches that can desorb PFAS without forming VOFs while preserving GAC's
44 structural and adsorptive properties are highly desirable. Several reported low-temperature
45 methods rely on organic solvents⁷⁻¹⁰ or aqueous solutions⁸. The application of these methods for
46 the desorption of long-chain (C-8) PFAS is challenging due to their strong affinity to surfaces,
47 and the large quantities of solvents required for GAC treatment hinder large-scale
48 implementation (Table S1).¹¹

49 Above its critical point (31°C, 7.4 MPa), CO₂ becomes a supercritical fluid (scCO₂)—a nonpolar
50 solvent with low dielectric constant and negligible molecular dipole moment.¹² Supercritical
51 fluid extraction (SFE) temperatures ($T < 100^\circ C$) would not trigger volatile fluorinated species
52 formation via thermal degradation.^{6, 13} SFE is used in commercial applications for removing

53 organics from solid matrices, e.g., botanical extraction, surface sterilization, food pasteurization,
54 and material synthesis.^{12, 14} In analytical chemistry, the SFE enables quantitative PAH recovery
55 from sorbent traps at $T = 45^\circ\text{C}$.¹⁵ There is also a report on scCO_2 use to extract PFOA and PFOS
56 from nonporous materials such as paper, fabrics, and sand.¹⁶
57 This study is the first investigation of low-temperature spent GAC regeneration using scCO_2
58 extraction with the addition of co-solvents and acid modifiers. Perfluorooctanoic acid (PFOA)
59 was chosen for this study due to its environmental persistence and high adsorption affinity, yet
60 our modified SFE approach yielded >99% desorption after 1 hour of GAC treatment.

61 2 METHODS AND MATERIALS

62 All chemicals and solvents used in this study are described in Section S1 in Supporting
63 Information (SI). The analytical methods for PFAS analysis are described in Section S2 in SI.
64 Each GAC sample was weighed (0.71 ± 0.01 g) and mixed with 19.0 mL of an aqueous solution
65 of PFOA at 20 ppm. After 5 days, the GAC was removed, and the liquid was analyzed using LC-
66 MS/MS. The GAC pellets were dried in an oven at 70°C for 12 hours. The spent GAC sub-
67 samples were extracted into 20 mL of ethanol (EtOH) + 0.15% NH_4OH solution¹¹ to determine
68 the amount of PFOA sorbed onto GAC. After 24 hours, the GAC was removed, and the liquid
69 was analyzed using LC-MS/MS.

70 Figure S1 describes the laboratory continuous flow reactor used in this study. The CO_2 from the
71 gas cylinder is condensed to the liquid phase in a calcium chloride cold bath (-10 to -5°C) CO_2
72 and pumped at 25 mL/min. The co-solvent (MeOH, or MeOH + 1% v/v H_2SO_4) injected at
73 1 mL/min, $T \sim 20^\circ\text{C}$, is mixed with scCO_2 before entering the reactor section. The CO_2 and
74 solvent post-mixing become a supercritical single-phase fluid if the organic solvent does not
75 exceed its solubility limit in the scCO_2 .¹⁷ $P = 20.3$ MPa, $T = 110 - 120^\circ\text{C}$ were chosen as the

76 operational parameters to satisfy single-phase conditions. After performing SFE for 60 minutes,
77 the column contents were dried in an oven at 70°C for 24 hours. The sample was divided into
78 two sub-samples: one was subjected to extraction by soaking in EtOH and ammonium
79 hydroxide, followed by LC-MS/MS; the other was loaded with PFOA again and underwent a
80 second regeneration cycle. Each experiment was performed in triplicates. The desorption
81 efficiency (DE) was calculated as:

$$82 \quad DE = \frac{[PFAS \in spent \ GAC] - [PFAS \in GAC \ after \ regeneration]}{[PFAS \in spent \ GAC]} \times 100 \%,$$

83 where $[PFAS \ in \ spent \ GAC]$ is the PFOA concentration (mg/g) in the spent sorbent, and $[PFAS$
84 $\ in \ GAC \ after \ regeneration]$ is the PFOA concentration (mg/g) in the regenerated sorbent.

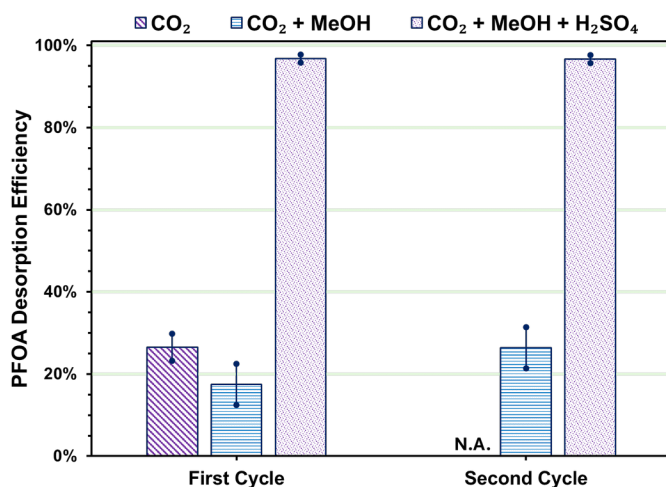
85 3 RESULTS AND DISCUSSION

86 3.1 Modified scCO₂ method for GAC regeneration

87 PFOA exhibits strong adsorption onto GAC due to hydrophobic and electrostatic interactions,
88 which present challenges for conventional techniques.¹⁸ The modified scCO₂ extraction yielded
89 near complete desorption of PFOA (Figure 1) by counteracting both forces. First, the method
90 takes advantage of the transition from a polar aqueous to a nonpolar scCO₂ environment, which
91 weakens/eliminates hydrophobic interactions. Once in scCO₂, PFOA miscibility decreases
92 compared to the shorter fluorinated molecules.¹⁹ Due to the high polarity of the
93 perfluorooctanoate ion, C₈F₁₅O₂⁻, electrostatic interactions become the dominant force; therefore,
94 in pure scCO₂, desorption efficiency was limited to < 30% (Figure 2).

95 The addition of organic co-solvents can enhance PFAS solubility in scCO₂. E.g., Chen et al.¹⁶
96 reported that the scCO₂/MeOH mixture was effective in extracting PFOA and PFOS from
97 nonporous materials. Table S1 shows that organic solvent-based extraction (MeOH, EtOH,

98 Acetone) in the batch GAC/ C-8 PFAS systems reach the DE ~ 40-95% after 12-24 hours.^{7, 8}
99 MeOH extraction showed the best results. Chularueangaksorn et al. utilized a column flow
100 reactor and MeOH, reporting DE = 67% desorption of PFOA from GAC 400 after 24 hours of
101 treatment.⁹ The solubility of PFAS in alcohols generally decreases for longer PFAS molecules
102 and longer carbon chain lengths of alcohol.²⁰ For example, the solubility of PFOS in MeOH is
103 ~ 37 g/L; it is ~ 5 times higher than in EtOH (~ 7 g/L). The solubility of PFOA in MeOH is
104 37.1 g/L, similar to PFOS's. Thus, in this proof-of-concept study, MeOH is used as a co-solvent.
105 In our experiment, adding MeOH alone did not significantly affect PFOA desorption (Figure 1),
106 indicating that scCO₂ is an effective agent for disrupting the hydrophobic interaction. A slight
107 increase in desorption efficiency from 18.7% to 26.3% in the second cycle might be attributed to
108 carryover from the previous cycle. While dipolar organic solvents can disrupt hydrophobic
109 interactions^{18, 21}, they are unlikely to affect the electrostatic interactions between PFAS
110 molecules and GAC surfaces.¹⁶ Lacking hydrophobic PFOA/GAC interaction in scCO₂ and
111 scCO₂/MeOH mixtures, the low desorption is contributed to electrostatic interactions, which can
112 be weakened by introducing an ionic agent. Thus, adding sulfuric acid (1% vol in MeOH)
113 increased the desorption efficiency to >97%.



114

115 **Figure 1.** PFOA desorption from GAC using only scCO₂, scCO₂ + MeOH, and scCO₂ + MeOH/H₂SO₄.
116 Experimental conditions are 110°C, 10 MPa, and an exposure time of 60 min. The second cycle of desorption in CO₂
117 was not conducted. Error bars are standard deviations from triplicated experiments.

118
119 The modified SFE regeneration method yielded significantly faster and more efficient PFAS
120 removal compared to conventional solvent-based techniques (Table S1). Treatment time was
121 1 hour, compared to 5-24 hours for traditional methods, yielding >97% PFAS removal (max
122 DE~99.9%). Notably, solvent consumption was decreased to ~ 4% of other reported solvent-
123 based methods, presenting an environmentally friendly and cost-effective approach for GAC
124 regeneration. The synergistic result of combining scCO₂, a co-solvent, and an acid modifier
125 achieves remarkable desorption results and complete restoration of GAC properties (Table 1).

126 3.2 Proposed mechanisms for modified supercritical CO₂ GAC regeneration

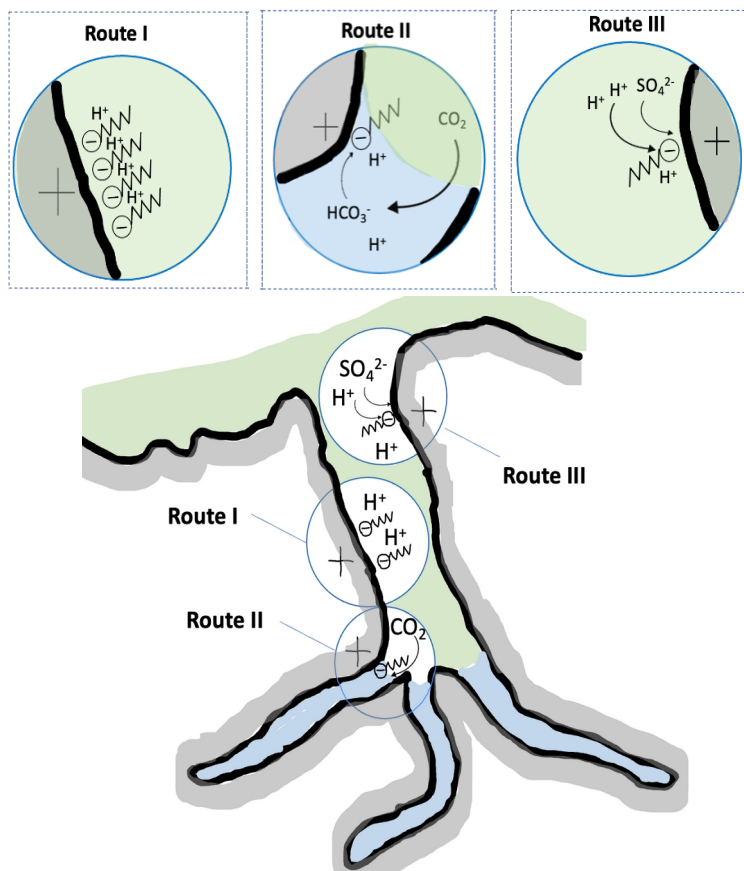
127 PFOA/GAC interaction is governed by two key forces, which must be effectively counteracted.
128 Specifically, the Filtrasorb 400 GAC has a point of zero charge (pH_{pzc}) of 8.65,¹ characteristic of
129 activated carbons with low oxygen content.²² The low oxygen content is reflected in the
130 measured concentration of oxygen-containing groups (phenolic, carboxylic, lactonic) of
131 0.21 mmol/g.²³ The measured pH during adsorption in this study (~ 4.8) was below the pH_{pzc}.
132 Under such conditions, the surface of the activated carbon becomes positively charged due to the
133 protonation of surface groups, enhancing electrostatic interactions with negatively charged PFAS
134 anions. The shift to the scCO₂ environment weakened hydrophobic interactions, leading to a
135 change from a predominantly surface-aligned orientation to a perpendicular orientation. This
136 reorientation, consistent with the classical work of Zisman and colleagues²⁴, minimizes the
137 contribution of hydrophobic forces, leaving electrostatic interactions as the dominant force
138 between the monovalent PFOA anion and the GAC surface in the scCO₂ environment.

139 **Route I** is enabled by the high dielectric permittivity of scCO_2 , facilitating proton availability
140 from PFOA dissociation. This can lead to the association of PFOA molecules (Figure 2, Route I)
141 and subsequent desorption in its protonated form. However, this route exhibits limited efficacy
142 for PFOA, $\text{DE} < 30\%$ (Figure 1). The effectiveness of this route may vary in other systems.

143 **Route II** involves the interaction of CO_2 molecules with water retained in the GAC pores,
144 leading to the formation of bicarbonate ions. While the bicarbonate ion is typically a weak
145 competitor for PFAS on GAC under normal conditions, the high concentration of CO_2 and small
146 pore volume may enhance the effect (Figure 2, Route II). However, the presence of water within
147 the pores can also promote hydrophobic interactions, potentially hindering the efficacy of Route
148 II.

149 **Route III** is based on disrupting the electrostatic forces between GAC and PFAS. The scCO_2 or
150 methanol cannot effectively weaken the electrostatic interaction between GAC and PFOA.
151 Figure 1 shows no significant change in desorption efficiency from scCO_2 to $\text{scCO}_2/\text{MeOH}$
152 experiments. On the other hand, adding the MeOH/acid mixture yields significant improvement
153 in the PFOA desorption. The MeOH assists in introducing sulfuric acid to a single-phase
154 supercritical mixture and ultimately inside the sorbent's pores. Mechanistically, a divalent sulfate
155 ion exhibits a stronger affinity to the active sites on the GAC surface, causing the release of a
156 weaker PFOA monovalent perfluorooctanoate ion, $\text{C}_8\text{F}_{15}\text{O}_2^-$ (Figure 2, Route III). Moreover,
157 sulfuric acid ($\text{pK}_a = -3$) can protonate PFOA ($\text{pK}_a = -0.2 - +3.8$).²⁵ The long-chain PFAS may
158 form micelles/hemi-micelles^{18, 26} in an aqueous environment that can interact with the GAC
159 surface during sorption; however, it is unclear if these structures interact in a $\text{scCO}_2/\text{organic}$ co-
160 solvent environment in the absence of liquid water. We expected that micelle formation is
161 negligible in a nonpolar solvent and does not significantly affect the proposed mechanism of

162 hydrophobic and electrostatic forces disruption in the $scCO_2$ environment. Though beyond the
 163 scope of the current report and the subject of ongoing work, we suspect that Route III should also
 164 hold for other PFAS.



165
 166 **Figure 2:** PFOA desorption routes from GAC, blue – porous water, green – $scCO_2$. Route I - in pure $scCO_2$, high
 167 dielectric permittivity and subsequent proton association lead to partial PFOA protonation; Route II - in pure $scCO_2$,
 168 bicarbonate ions formed from CO_2 interaction with retained water compete with PFOA for adsorption sites; Route
 169 III - in $scCO_2/ MeOH/ H_2SO_4$ (i) competition of the sulfate ion for GAC active site and (ii) PFOA protonation.

170

171 3.3 Impacts of co-solvent concentration on regeneration efficiency

172 Increasing the concentration of acid-modified co-solvent in $scCO_2$ yielded the highest desorption
 173 efficiency of 99.9% (Figure S2). In these experiments, the CO_2 flow rate was constant
 174 (25 mL/min), and the co-solvent flow rate varied from 0.2 to 6.8 mL/min. The results showed
 175 only marginal improvement for high MeOH flow rates. This corroborates that the hydrophobic
 176 interaction does not play a significant role in the $scCO_2$ environment, and the disruption of

177 electrostatic attraction by the pH surface modifier is the dominant mechanism. Further research
178 is needed to optimize the acid concentration in the scCO₂/ MeOH mixture and substitute MeOH
179 with more environmentally friendly solvents.

180 From a practical perspective, these observations suggest that the process can yield a very
181 concentrated effluent, reducing consumption of co-solvent and, in turn, reducing the volume of
182 effluent that needs to be treated in the end-of-life destruction step. In a binary CO₂/ solvent
183 system, the pressure, temperature, and mole fractions of each solvent determine the phase of the
184 overall fluid mixture. Based on data extrapolation from Reighard et al.²⁷, at $X_{MeOH}=0.1792$ and
185 10 MPa, the dew point of the CO₂/ MeOH mixture is at ~ 110°C. Assuming that a trace
186 concentration of sulfuric acid does not affect the solubility of MeOH in CO₂, a lower X_{MeOH}
187 would lead to a single-phase supercritical gas-like mixture of MeOH completely dissolved in
188 CO₂, while a higher X_{MeOH} would lead to a two-phase mixture of liquid MeOH and the gas-like
189 scCO₂. Adjusting the flow rates controls MeOH concentration and mixture phase during
190 regeneration. Though limiting the concentration of MeOH produces more concentrated effluent,
191 the presence of a liquid interface at the GAC surface may improve the desorption and
192 regeneration efficiency, as seen in the experiment at 6.8 mL/min, where the experimental
193 condition was close to the MeOH dew point.

194 **3.4 Assessment of GAC properties after regeneration**

195 A sustainable PFAS regeneration approach must also maintain GAC's structural integrity and
196 adsorption capacity after regeneration. Table 1 shows that BET surface area and micropore
197 volume of spent GAC decreased (971 to 922 m²/g), indicating the occupation of active sorption
198 sites and pore blockage by PFOA molecules. After the regeneration step, the BET surface area
199 and micropore volume slightly increased (971 to 1012 m²/g) compared to the virgin GAC.

200 Though it is unclear what fraction of PFOA molecules resided within the micropores or on the
201 surface, the modified SFE could desorb PFOA from all active sites, preserving the GAC porous
202 structure. The adsorption capacity of regenerated GAC was 0.52 ± 0.02 mg/g—nearly identical
203 to the virgin GAC. We inferred that sulfate ions that competed with the $C_8F_{15}O_2^-$ ion in the $scCO_2$
204 environment entered the aqueous phase during the next adsorption cycle, allowing reuse of
205 regenerated GAC.

206 **Table 1: Characteristics of the porous structure of virgin GAC, PFOA-laden GAC, and regenerated GAC**

| | Virgin GAC | PFOA-laden GAC | Regenerated GAC |
|--|------------|----------------|-----------------|
| BET Surface Area (m ² /g) | 973.1 | 922.1 | 1012.2 |
| Micropore Surface Area (m ² /g) | 573.7 | 544.3 | 609.8 |
| Micropore Volume (cm ³ /g) | 0.287 | 0.271 | 0.299 |

207 **4 Environmental Implications**

208 Traditional waste management approaches often involve the disposal of contaminated
209 adsorbents, leading to substantial environmental and economic burdens. This unsustainable
210 practice necessitates the development of efficient and environmentally friendly spent sorbent
211 regeneration approaches. Our $scCO_2$ -based sorbent regeneration method holds significant
212 promise for mitigating the environmental impact of PFAS contamination, offering a sustainable
213 alternative to traditional practices. Mild temperature conditions minimize energy consumption
214 and reduce the risk of sorbent degradation. Though the CO_2 was naturally aspirated during the
215 experiment, it can be captured and reused in practical applications. After dropping the
216 temperature and pressure below supercritical conditions, the MeOH, H_2SO_4 , and PFOA mixture
217 naturally separates to form a concentrated liquid effluent.

218 The modified SFE process offers significant environmental benefits. The need for disposal is
219 minimized by regenerating the GAC, reducing landfill waste, and reducing the associated
220 environmental impact. Reusable GAC practices lessen the demand for new materials, promoting

221 resource conservation and minimizing the environmental impact of production. Furthermore, the
222 process produces a concentrated PFAS effluent, facilitating efficient and cost-effective
223 downstream end-of-life PFAS (and other contaminant) destruction. Future research should focus
224 on expanding the applicability of this method to a broader range of PFAS compounds and
225 optimizing operational parameters (e.g., temperature, exposure time, and co-solvent
226 formulation). The potential of this approach extends beyond GAC regeneration, with
227 applications for other sorbents, such as ion-exchange resins.

228 **Supporting Information –**

229 S1. Experimental setup, chemicals, and reagents

230 S2. Analytical method

231 **Disclaimer** – This document has been subjected to the U.S. Environmental Protection Agency's
232 review and has been approved for publication. The research presented was not performed or
233 funded by the EPA and was not subject to the EPA's quality system requirements. The views
234 expressed in this article are those of the authors and do not necessarily represent the views or
235 policies of the Agency. The Agency does not endorse any commercial products, services, or
236 enterprises.

237 **References**

238 (1) Zhang, Y.; Thomas, A.; Apul, O.; Venkatesan, A. K. Coexisting ions and long-chain per- and
239 polyfluoroalkyl substances (PFAS) inhibit the adsorption of short-chain PFAS by granular
240 activated carbon. *Journal of Hazardous Materials* **2023**, *460*, 132378. DOI:
241 <https://doi.org/10.1016/j.jhazmat.2023.132378>.

242 (2) Vakili, M.; Cagnetta, G.; Deng, S.; Wang, W.; Gholami, Z.; Gholami, F.; Dastyar, W.;
243 Mojiri, A.; Blaney, L. Regeneration of exhausted adsorbents after PFAS adsorption: A critical
244 review. *Journal of Hazardous Materials* **2024**, *471*, 134429. DOI:
245 <https://doi.org/10.1016/j.jhazmat.2024.134429>. Gagliano, E.; Falciglia, P. P.; Zaker, Y.; Birben,
246 N. C.; Karanfil, T.; Roccaro, P. State of the research on regeneration and reactivation techniques
247 for per- and polyfluoroalkyl substances (PFAS)-laden granular activated carbons (GACs).
248 *Current Opinion in Chemical Engineering* **2023**, *42*, 100955. DOI:
249 <https://doi.org/10.1016/j.coche.2023.100955>.

250 (3) Ellis, A. C.; Boyer, T. H.; Fang, Y.; Liu, C. J.; Strathmann, T. J. Life cycle assessment and
251 life cycle cost analysis of anion exchange and granular activated carbon systems for remediation

252 of groundwater contaminated by per- and polyfluoroalkyl substances (PFASs). *Water Research*
253 **2023**, 243, 120324. DOI: <https://doi.org/10.1016/j.watres.2023.120324>.
254 (4) Smith, S. J.; Lewis, J.; Wiberg, K.; Wall, E.; Ahrens, L. Foam fractionation for removal of
255 per- and polyfluoroalkyl substances: Towards closing the mass balance. *Science of The Total*
256 *Environment* **2023**, 871, 162050. DOI: <https://doi.org/10.1016/j.scitotenv.2023.162050>. Lin, H.;
257 Lao, J.-Y.; Wang, Q.; Ruan, Y.; He, Y.; Lee, P. K. H.; Leung, K. M. Y.; Lam, P. K. S. Per- and
258 polyfluoroalkyl substances in the atmosphere of waste management infrastructures: Uncovering
259 secondary fluorotelomer alcohols, particle size distribution, and human inhalation exposure.
260 *Environment International* **2022**, 167, 107434. DOI:
261 <https://doi.org/10.1016/j.envint.2022.107434>.
262 (5) Sahu, S. P.; Qanbarzadeh, M.; Ateia, M.; Torkzadeh, H.; Maroli, A. S.; Cates, E. L. Rapid
263 degradation and mineralization of perfluorooctanoic acid by a new petitjeanite Bi₃O(OH)(PO₄)₂
264 microparticle ultraviolet photocatalyst. *Environmental Science & Technology Letters* **2018**, 5
265 (8), 533-538. Kalra, S. S.; Cranmer, B.; Dooley, G.; Hanson, A. J.; Maraviov, S.; Mohanty, S.
266 K.; Blotevogel, J.; Mahendra, S. Sonolytic destruction of Per-and polyfluoroalkyl substances in
267 groundwater, aqueous Film-Forming Foams, and investigation derived waste. *Chem. Eng. J.*
268 **2021**, 425, 131778. Singh, R. K.; Fernando, S.; Baygi, S. F.; Multari, N.; Thagard, S. M.;
269 Holsen, T. M. Breakdown products from perfluorinated alkyl substances (PFAS) degradation in
270 a plasma-based water treatment process. *Environ. Sci. Technol.* **2019**, 53 (5), 2731-2738. DOI:
271 10.1021/acs.est.8b07031. Smith, S. J.; Lauria, M.; Ahrens, L.; McCleaf, P.; Hollman, P.;
272 Bjälkefur Seroka, S.; Hamers, T.; Arp, H. P. H.; Wiberg, K. Electrochemical Oxidation for
273 Treatment of PFAS in Contaminated Water and Fractionated Foam— A Pilot-Scale Study. *ACS*
274 *Es&t Water* **2023**, 3 (4), 1201-1211. Austin, C.; Li, J.; Moore, S.; Purohit, A.; Pinkard, B. R.;
275 Novosselov, I. V. Destruction and defluorination of PFAS matrix in continuous-flow
276 supercritical water oxidation reactor: Effect of operating temperature. *Chemosphere* **2023**, 327,
277 138358. Li, J.; Pinkard, B. R.; Wang, S.; Novosselov, I. V. Review: Hydrothermal treatment of
278 per- and polyfluoroalkyl substances (PFAS). *Chemosphere* **2022**, 307, 135888. DOI:
279 <https://doi.org/10.1016/j.chemosphere.2022.135888>. Yang, N.; Yang, S.; Ma, Q.; Beltran, C.;
280 Guan, Y.; Morsey, M.; Brown, E.; Fernando, S.; Holsen, T. M.; Zhang, W. Solvent-Free
281 Nonthermal Destruction of PFAS Chemicals and PFAS in Sediment by Piezoelectric Ball
282 Milling. *Environmental Science & Technology Letters* **2023**, 10 (2), 198-203. Li, J.; Austin, C.;
283 Moore, S.; Pinkard, B. R.; Novosselov, I. V. PFOS destruction in a continuous supercritical
284 water oxidation reactor. *Chem. Eng. J.* **2023**, 451, 139063. Hori, H.; Nagaoka, Y.; Sano, T.;
285 Kutsuna, S. Iron-induced decomposition of perfluorohexanesulfonate in sub- and supercritical
286 water. *Chemosphere* **2008**, 70 (5), 800-806. DOI: 10.1016/j.chemosphere.2007.07.015. Wu, B.
287 R.; Hao, S. L.; Choi, Y. J.; Higgins, C. P.; Deeb, R.; Strathmann, T. J. Rapid Destruction and
288 Defluorination of Perfluorooctanesulfonate by Alkaline Hydrothermal Reaction. *Environmental*
289 *Science & Technology Letters* **2019**, 6 (10), 630-636. DOI: 10.1021/acs.estlett.9b00506. Pinkard,
290 B. R.; Shetty, S.; Stritzinger, D.; Bellona, C.; Novosselov, I. V. Destruction of
291 perfluorooctanesulfonate (PFOS) in a batch supercritical water oxidation reactor. *Chemosphere*
292 **2021**, 279, 130834. Pinkard, B. R. Aqueous film-forming foam treatment under alkaline
293 hydrothermal conditions. *Journal of Environmental Engineering* **2022**, 148 (2), 05021007. Hao,
294 S.; Choi, Y.-J.; Wu, B.; Higgins, C. P.; Deeb, R.; Strathmann, T. J. Hydrothermal Alkaline
295 Treatment for Destruction of Per- and Polyfluoroalkyl Substances in Aqueous Film-Forming
296 Foam. *Environmental Science & Technology* **2021**, 55 (5), 3283-3295. DOI:
297 10.1021/acs.est.0c06906. Soker, O.; Hao, S.; Trewyn, B. G.; Higgins, C. P.; Strathmann, T. J.

298 Application of Hydrothermal Alkaline Treatment to Spent Granular Activated Carbon:
299 Destruction of Adsorbed PFASs and Adsorbent Regeneration. *Environmental Science &*
300 *Technology Letters* **2023**, 10 (5), 425-430. DOI: 10.1021/acs.estlett.3c00161. Hao, S.; Choi, Y.
301 J.; Deeb, R. A.; Strathmann, T. J.; Higgins, C. P. Application of Hydrothermal Alkaline
302 Treatment for Destruction of Per- and Polyfluoroalkyl Substances in Contaminated Groundwater
303 and Soil. *Environmental Science & Technology* **2022**, 56 (10), 6647-6657. DOI:
304 10.1021/acs.est.2c00654. Hao, S.; Reardon, P. N.; Choi, Y. J.; Zhang, C.; Sanchez, J. M.;
305 Higgins, C. P.; Strathmann, T. J. Hydrothermal Alkaline Treatment (HALT) of Foam
306 Fractionation Concentrate Derived from PFAS-Contaminated Groundwater. *Environmental*
307 *Science & Technology* **2023**, 57 (44), 17154-17165. DOI: 10.1021/acs.est.3c05140. Endo, J.;
308 Funazukuri, T. Hydrothermal alkaline defluorination rate of perfluorocarboxylic acids (PFCAs).
309 *Journal of Chemical Technology & Biotechnology* **2023**, 98 (5), 1215-1221. Pinkard, B. R.;
310 Austin, C.; Purohit, A. L.; Li, J.; Novosselov, I. V. Destruction of PFAS in AFFF-impacted fire
311 training pit water, with a continuous hydrothermal alkaline treatment reactor. *Chemosphere*
312 **2023**, 314, 137681.

313 (6) Austin, C.; Purohit, A. L.; Thomsen, C.; Pinkard, B. R.; Strathmann, T. J.; Novosselov, I. V.
314 Hydrothermal Destruction and Defluorination of Trifluoroacetic Acid (TFA). *Environmental*
315 *Science & Technology* **2024**. DOI: 10.1021/acs.est.3c09404.

316 (7) Du, Z.; Deng, S.; Liu, D.; Yao, X.; Wang, Y.; Lu, X.; Wang, B.; Huang, J.; Wang, Y.; Xing,
317 B.; et al. Efficient adsorption of PFOS and F53B from chrome plating wastewater and their
318 subsequent degradation in the regeneration process. *Chemical Engineering Journal* **2016**, 290,
319 405-413. DOI: <https://doi.org/10.1016/j.cej.2016.01.077>.

320 (8) Deng, S.; Nie, Y.; Du, Z.; Huang, Q.; Meng, P.; Wang, B.; Huang, J.; Yu, G. Enhanced
321 adsorption of perfluorooctane sulfonate and perfluorooctanoate by bamboo-derived granular
322 activated carbon. *Journal of Hazardous Materials* **2015**, 282, 150-157. DOI:
323 <https://doi.org/10.1016/j.jhazmat.2014.03.045>.

324 (9) Chularueangaksorn, P.; Tanaka, S.; Fujii, S.; Kunacheva, C. Adsorption of perfluorooctanoic
325 acid (PFOA) onto anion exchange resin, non-ion exchange resin, and granular-activated carbon
326 by batch and column. *Desalination and Water Treatment* **2014**, 52 (34-36), 6542-6548. DOI:
327 10.1080/19443994.2013.815589.

328 (10) Senevirathna, S. T. M. L. D.; Tanaka, S.; Fujii, S.; Kunacheva, C.; Harada, H.; Ariyadasa,
329 B. H. A. K. T.; Shivakoti, B. R. Adsorption of perfluorooctane sulfonate (n-PFOS) onto non ion-
330 exchange polymers and granular activated carbon: Batch and column test. *Desalination* **2010**,
331 260 (1), 29-33. DOI: <https://doi.org/10.1016/j.desal.2010.05.005>.

332 (11) Siriwardena, D. P.; James, R.; Dasu, K.; Thorn, J.; Iery, R. D.; Pala, F.; Schumitz, D.;
333 Eastwood, S.; Burkitt, N. Regeneration of per- and polyfluoroalkyl substance-laden granular
334 activated carbon using a solvent based technology. *Journal of Environmental Management* **2021**,
335 289, 112439. DOI: <https://doi.org/10.1016/j.jenvman.2021.112439>.

336 (12) Beckman, E. J. Supercritical and near-critical CO₂ in green chemical synthesis and
337 processing. *The Journal of Supercritical Fluids* **2004**, 28 (2), 121-191. DOI:
338 [https://doi.org/10.1016/S0896-8446\(03\)00029-9](https://doi.org/10.1016/S0896-8446(03)00029-9).

339 (13) Verma, S.; Lee, T.; Sahle-Demessie, E.; Ateia, M.; Nadagouda, M. N. Recent advances on
340 PFAS degradation via thermal and nonthermal methods. *Chemical Engineering Journal*
341 *Advances* **2023**, 13, 100421. DOI: <https://doi.org/10.1016/j.cej.2022.100421>.

342 (14) Schantz, M. M.; Chesler, S. Supercritical fluid extraction procedure for the removal of trace
343 organic species from solid samples. *J. Chromatogr. A* **1986**, 363 (2), 397-401. López-Periago,

344 A.; Vallcorba, O.; Frontera, C.; Domingo, C.; Ayllón, J. A. Exploring a novel preparation
345 method of 1D metal organic frameworks based on supercritical CO₂. *Dalton Transactions* **2015**,
346 *44* (16), 7548-7553, 10.1039/C5DT00521C. DOI: 10.1039/C5DT00521C. López-Periago, A. M.;
347 Portoles-Gil, N.; López-Domínguez, P.; Fraile, J.; Saurina, J.; Aliaga-Alcalde, N.; Tobias, G.;
348 Ayllón, J. A.; Domingo, C. Metal–Organic Frameworks Precipitated by Reactive Crystallization
349 in Supercritical CO₂. *Crystal Growth & Design* **2017**, *17* (5), 2864-2872. DOI:
350 10.1021/acs.cgd.7b00378. Portolés-Gil, N.; Gowing, S.; Vallcorba, O.; Domingo, C.; López-
351 Periago, A. M.; Ayllón, J. A. Supercritical CO₂ utilization for the crystallization of 2D metal-
352 organic frameworks using tert-butylpyridine additive. *Journal of CO₂ Utilization* **2018**, *24*, 444-
353 453. DOI: <https://doi.org/10.1016/j.jcou.2018.02.004>. Kubovics, M.; Rojas, S.; López, A. M.;
354 Fraile, J.; Horcajada, P.; Domingo, C. Fully supercritical CO₂ preparation of a nanostructured
355 MOF composite with application in cutaneous drug delivery. *The Journal of Supercritical Fluids*
356 **2021**, *178*, 105379. DOI: <https://doi.org/10.1016/j.supflu.2021.105379>.
357 (15) Hawthorne, S. B.; Miller, D. J. Extraction and recovery of organic pollutants from
358 environmental solids and Tenax-GC using supercritical CO₂. *J. Chromatogr. Sci.* **1986**, *24* (6),
359 258-264.
360 (16) Chen, H.-Y.; Liao, W.; Wu, B.-Z.; Nian, H.; Chiu, K.; Yak, H.-K. Removing
361 perfluorooctane sulfonate and perfluorooctanoic acid from solid matrices, paper, fabrics, and
362 sand by mineral acid suppression and supercritical carbon dioxide extraction. *Chemosphere*
363 **2012**, *89* (2), 179-184. DOI: <https://doi.org/10.1016/j.chemosphere.2012.06.003>.
364 (17) Wu, W.; Ke, J.; Poliakoff, M. Phase Boundaries of CO₂ + Toluene, CO₂ + Acetone, and
365 CO₂ + Ethanol at High Temperatures and High Pressures. *Journal of Chemical & Engineering*
366 *Data* **2006**, *51* (4), 1398-1403. DOI: 10.1021/je060099a. Chatwell, R. S.; Guevara-Carrion, G.;
367 Gaponenko, Y.; Shevtsova, V.; Vrabec, J. Diffusion of the carbon dioxide–ethanol mixture in the
368 extended critical region. *Physical Chemistry Chemical Physics* **2021**, *23* (4), 3106-3115,
369 10.1039/D0CP04985A. DOI: 10.1039/D0CP04985A.
370 (18) Du, Z.; Deng, S.; Bei, Y.; Huang, Q.; Wang, B.; Huang, J.; Yu, G. Adsorption behavior and
371 mechanism of perfluorinated compounds on various adsorbents—A review. *Journal of*
372 *Hazardous Materials* **2014**, *274*, 443-454. DOI: <https://doi.org/10.1016/j.jhazmat.2014.04.038>.
373 (19) Dardin, A.; DeSimone, J. M.; Samulski, E. T. Fluorocarbons dissolved in supercritical
374 carbon dioxide. NMR evidence for specific solute– solvent interactions. *The Journal of Physical*
375 *Chemistry B* **1998**, *102* (10), 1775-1780.
376 (20) Meng, P.; Deng, S.; Du, Z.; Wang, B.; Huang, J.; Wang, Y.; Yu, G.; Xing, B. Effect of
377 hydro-oleophobic perfluorocarbon chain on interfacial behavior and mechanism of
378 perfluorooctane sulfonate in oil-water mixture. *Scientific Reports* **2017**, *7* (1), 44694. DOI:
379 10.1038/srep44694.
380 (21) Dutta, T.; Kim, T.; Vellingiri, K.; Tsang, D. C. W.; Shon, J. R.; Kim, K.-H.; Kumar, S.
381 Recycling and regeneration of carbonaceous and porous materials through thermal or solvent
382 treatment. *Chemical Engineering Journal* **2019**, *364*, 514-529. DOI:
383 <https://doi.org/10.1016/j.cej.2019.01.049>.
384 (22) Morlay, C.; Quivet, E.; Pilshofer, M.; Faure, R.; Joly, J.-P. Adsorption of Imazamox
385 herbicide onto Filtrasorb 400 activated carbon. *Journal of Porous Materials* **2012**, *19* (1), 79-86.
386 DOI: 10.1007/s10934-011-9450-4.
387 (23) Liu Mei, Y.; Tsang Daniel, C.; Hu, J.; Ng Kelvin, T.; Liu, T.; Lo Irene, M. Adsorption of
388 Methylene Blue and Phenol by Wood Waste Derived Activated Carbon. *Journal of*

389 *Environmental Engineering* **2008**, 134 (5), 338-345. DOI: 10.1061/(ASCE)0733-
390 9372(2008)134:5(338) (accessed 2024/05/15).
391 (24) Shafrin, E. G.; Zisman, W. A. Effect of Progressive Fluorination of a Fatty Acid on the
392 Wettability of its Adsorbed Monolayer. *The Journal of Physical Chemistry* **1962**, 66 (4), 740-
393 748. DOI: 10.1021/j100810a039.
394 (25) Burns, D. C.; Ellis, D. A.; Li, H.; McMurdo, C. J.; Webster, E. Experimental pKa
395 Determination for Perfluorooctanoic Acid (PFOA) and the Potential Impact of pKa
396 Concentration Dependence on Laboratory-Measured Partitioning Phenomena and Environmental
397 Modeling. *Environmental Science & Technology* **2008**, 42 (24), 9283-9288. DOI:
398 10.1021/es802047v.
399 (26) Uriakhil, M. A.; Sidnell, T.; De Castro Fernández, A.; Lee, J.; Ross, I.; Bussemaker, M. Per-
400 and poly-fluoroalkyl substance remediation from soil and sorbents: A review of adsorption
401 behaviour and ultrasonic treatment. *Chemosphere* **2021**, 282, 131025. DOI:
402 <https://doi.org/10.1016/j.chemosphere.2021.131025>.
403 (27) Reighard, T. S.; Lee, S. T.; Olesik, S. V. Determination of methanol/CO₂ and
404 acetonitrile/CO₂ vapor-liquid phase equilibria using a variable-volume view cell. *Fluid Phase*
405 *Equilibria* **1996**, 123 (1-2), 215-230.
406

407

408

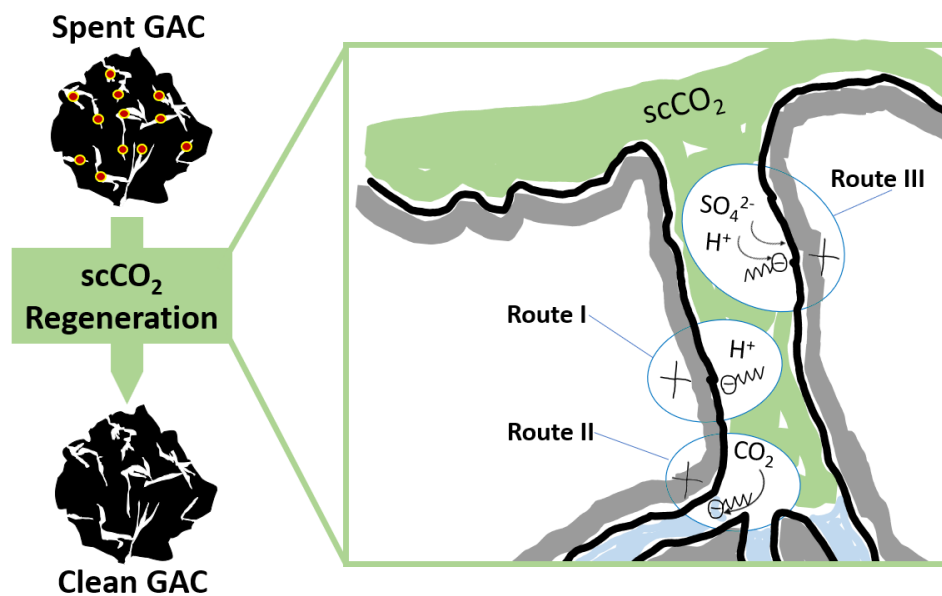
409

410

411

412

413 Graphical abstract:



414

415